Eyes on the future – evidence for trade-offs between growth, storage and defense in Norway spruce

Authors:

Jianbei Huang [1], Almuth Hammerbacher [2,4], Alexander Weinhold [3], Michael Reichelt [2], Gerd Gleixner [1], Thomas Behrendt [1], Nicole M. van Dam [3,5], Anna Sala [6], Jonathan Gershenzon[2], Susan Trumbore[1] and Henrik Hartmann [1]

Affiliations:

[1] Max Planck Institute for Biogeochemistry, Hans-Knöll-Str. 10, 07745 Jena, Germany

2 Max Planck Institute for Chemical Ecology, Hans-Knöll-Str. 8, 07745 Jena, Germany

[3] German Centre for Integrative Biodiversity Research, Deutscher Platz 5e, 04103 Leipzig, Germany

[4] Forestry and Agricultural Biotechnology Institute, Department of Zoology and Entomology, University of Pretoria, Private Bag X20, 0028 Pretoria, South Africa

[5] Institute of Biodiversity, Friedrich Schiller University, Dornburger-Str. 159, 07743 Jena, Germany

[6] Division of Biological Sciences, The University of Montana, Missoula, 59812 MT, USA

Author for correspondence: Jianbei Huang

Tel: +49 3641 576150

Email: hjianbei@bgc-jena.mpg.de

ORCID IDs:

Jianbei Huang: http://orcid.org/0000-0001-5286-5645

Almuth Hammerbacher: http://orcid.org/0000-0002-0262-2634

Alexander Weinhold: http://orcid.org/0000-0003-1418-7788

Gerd Gleixner: http://orcid.org/0000-0002-4616-0953

Nicole M. van Dam: http://orcid.org/0000-0003-2622-5446

Jonathan Gershenzon: http://orcid.org/0000-0002-1812-1551

Susan Trumbore: http://orcid.org/0000-0003-3885-6202

Henrik Hartmann: http://orcid.org/0000-0002-9926-5484

Total words: 6564; Introduction: 1239; Materials and Methods: 1795; Results: 1319; Discussion: 1864; Conclusion and Outlook: 267; Acknowledgements: 80

Tables and figures in main body: 0 tables and 9 figures

Supporting Information: 1 method, 2 table and 5 figures

Summary

- Carbon (C) allocation plays a central role in tree responses to environmental changes. Yet, fundamental questions remain about how trees allocate C to different sinks, for example, growth versus storage and defense.
- To elucidate allocation priorities, we manipulated the whole-tree C balance by modifying atmospheric CO_2 concentrations ($[CO_2]$) to create two distinct gradients of declining C availability, and compared how C was allocated among fluxes (respiration and volatile monoterpenes) and biomass C pools (total biomass, non-structural carbohydrates (NSC) and secondary metabolites (SM)) in well-watered Norway spruce (*Picea abies*) saplings. Continuous isotope labelling was used to trace the fate of newly-assimilated C.
- Reducing $[CO_2]$ to 120 ppm caused an aboveground C compensation point (*i.e.* net C balance was zero) and resulted in decreases in growth and respiration. By contrast, soluble sugars and SM remained relatively constant in aboveground young organs and were partially maintained with a constant allocation of newly-assimilated C, even at expense of root death from C exhaustion.
- We conclude that spruce trees have a conservative allocation strategy under source limitation: growth and respiration can be down-regulated to maintain 'operational' levels of NSC while investing newly-assimilated C into future survival by producing SM.

Key words: biogenic volatile organic compounds; carbon allocation; carbon limitation; CO_2; growth-defense trade-offs; nonstructural carbohydrate storage; Norway spruce (*Picea abies*); secondary metabolites

Introduction

Trees are long-lived sessile organisms that adjust their metabolic processes to survive under a rapidly changing climate (Trumbore *et al.*, 2015). Carbon (C) plays a fundamental role in plant metabolism due to its ability to bond with hydrogen and oxygen, as well as many other elements, to form primary and secondary metabolites (SM). Thus, studying 'the fate of C' in plant metabolism is crucial for understanding tree responses to environmental change (Atkin, 2015). C allocation is thought to be driven by the C balance between supply (source) and demand (sink). Changes in resource availability such as CO_2, light, temperature, nutrients and water (Fatichi *et al.*, 2014), may in turn influence source and sink activity and thus indirectly control plant C allocation. Of particular interest is the atmospheric CO_2 concentration ($[CO_2]$) which directly influences source activity but not sink activity. Manipulations of $[CO_2]$ thus allow investigations on the roles of source activity in C allocation relative to other limiting factors. For example, at high $[CO_2]$, when C is non-limiting, growth may be limited by the availability of nutrients (Lewis *et al.*, 2010; Reich *et al.*, 2014) or water (Reich *et al.*, 2014; Faralli *et al.*, 2017). By contrast, at low $[CO_2]$, photosynthesis and growth are strongly C-limited (Lewis *et al.*, 2010; Schmid *et al.*, 2017). The latter has been the case in trees under preindustrial levels of 280 ppm $[CO_2]$ or glacial maximum levels of 170 ppm $[CO_2]$ (Gerhart *et al.*, 2012), and the exposure and survival of trees during low CO_2 periods suggests strong ability to optimize C allocation strategies. However, it remains unclear how changing $[CO_2]$ and resulting alteration of C availability may alter plant allocation strategies, e.g., whether allocation to storage and defence that are essential for survival comes at the cost of other sinks like growth and its associated respiratory requirements. Such information will provide mechanistic insight into plant response to C availability under the influences of environmental constraints (e.g. long-term severe drought, cold and shading) as well as of biotic stress.

Nonstructural carbohydrates (NSC) are primary metabolites and serve multiple functions such as storage, transport of C (and energy) and osmotic adjustment (Dietze *et al.*, 2014; Hartmann & Trumbore, 2016). Moderate C limitation induced by reducing $[CO_2]$ to 280 ppm (Ayub *et al.*, 2011) or 170 ppm (Huang *et al.*, 2017a) decreased total NSC (in particular starch)

while respiration rate remained constant, indicating that NSC are remobilized to meet respiratory demand. By contrast, under extremely limiting [CO_2] (40 ppm, Hartmann *et al.*, 2013) and under complete shading (Sevanto *et al.*, 2014; Fischer *et al.*, 2015), respiration decreased over time along with NSC reserves, suggesting respiration may be down-regulated to reduce the consumption of NSC storage and thereby prolong survival. Hence, respiration can be fuelled by NSC storage but only up to a threshold below which long-term survival is at risk. Similarly, there has been an active debate about whether growth can be limited by NSC storage in order to ensure future survival under drought and cold stress (Sala *et al.*, 2012; Wiley & Helliker, 2012; Palacio *et al.*, 2014). Drought and cold decrease growth (C demand) earlier and to a greater degree than photosynthesis (C supply). This leads plants to accumulate C which is stored as NSC pools through an 'overflow' mechanism – *i.e*. when C is available in excess of sink demands (*sensu* accumulation, Chapin *et al.*, 1990). By contrast, recent studies provided evidence that NSC may be prioritized over growth under defoliation (Wiley *et al.*, 2017a), drought (Galiano *et al.*, 2017) and low [CO_2] (Hartmann *et al.*, 2015), suggesting a trade-off between storage and growth (*sensu* reserve formation, Chapin *et al.*, 1990).

Secondary metabolites (SM) are compounds not directly involved in primary metabolic activities (e.g. growth and reproduction). Often SM fulfil important functions such as detoxification (Neilson *et al.*, 2013), anti-herbivore (Mithöfer & Boland, 2012) and anti-pathogen defense (Ullah *et al.*, 2017; Hammerbacher *et al.*, 2018). The biosynthesis of these compounds may be costly when resources are limited because they divert resources away from other sinks, such as growth. An assumption of the C-nutrient balance hypothesis (Bryant *et al.*, 1983) and the growth-differentiation balance hypothesis (Herms & Mattson, 1992) is that allocation to SM depends on the availability of NSC, which in turn depends on resource availability and C/N balance. They postulate that the process is driven by the balance between C supply via photosynthesis and C demand for growth. Such hypotheses are supported by the decrease in SM under shading (Roberts & Paul, 2006). However, shading results in negative C balance where growth is also strongly limited, making it difficult to determine the trade-offs between SM and growth. In addition, shading may also stimulate growth (*i.e.* allocation) via phytochromes (Casal, 2013) and thus suppress SM production, independent of C availability.

Unlike SM stored in tissues, responses of volatile SM (including isoprene and terpenoids) to changes in C availability have received less attention. This is despite the fact that they represent a considerable C investment to the plant and play important roles in protection against oxidants (Vickers *et al.*, 2009) and herbivory (Unsicker *et al.*, 2009). It is established that reducing atmospheric [CO_2] stimulates isoprene emissions (Way *et al.*, 2013). This is likely because ATP and NADPH may exceed the demands for Calvin cycle and thus reduce more carbohydrates to isoprene precursor, dimethylallyl diphosphate (Harrison *et al.*, 2013). However, it remains unclear how changes in C availability may influence emissions of monoterpenes. Given that the isoprene precursor is also used for monoterpene synthesis (Vickers *et al.*, 2009), we may expect similar effects on monoterpene emissions.

Our study aims to elucidate C allocation priorities in trees via reducing C availability. Reducing [CO_2] has been suggested to be a good approach for manipulating whole-plant C balance (Hartmann & Trumbore, 2016) without causing artificial effects on sink activities as compared to shading and defoliation. For example, severe defoliation may induce synthesis of defence compounds (Massad *et al.*, 2014), independent of C availability. We therefore exposed plants to a gradient of atmospheric [CO_2] (400, 280, 170, 120 and 50 ppm) in a step-wise fashion (Fig. **1a**), and measured whole-plant C fluxes (assimilation, respiration and volatile monoterpenes) and biomass partitioning (structural biomass, NSC and SM). Continuous isotope labelling was applied to trace the allocation of the C assimilated during reduced [CO_2] into C sinks, *i.e.* growth, soluble sugars and phenolic compounds. We assume that pools with higher allocation priority will decline less than those with lower priority under C limitation. We also assume that any NSC and SM found in dead organs are inaccessible pools regardless of C availability.

The plant chosen for our experiments is Norway spruce (*Picea abies* L.), which survived ice age conditions in the refugia of Scandinavia (Parducci *et al.*, 2012). Given its potential longevity, we hypothesize that Norway spruce may have a conservative allocation strategy that prioritizes NSC and SM over other sinks (e.g. growth and respiration) to ensure survival during periodic stresses such as shading, defoliation and drought. Specifically, we hypothesize that (see Fig. **1b**):

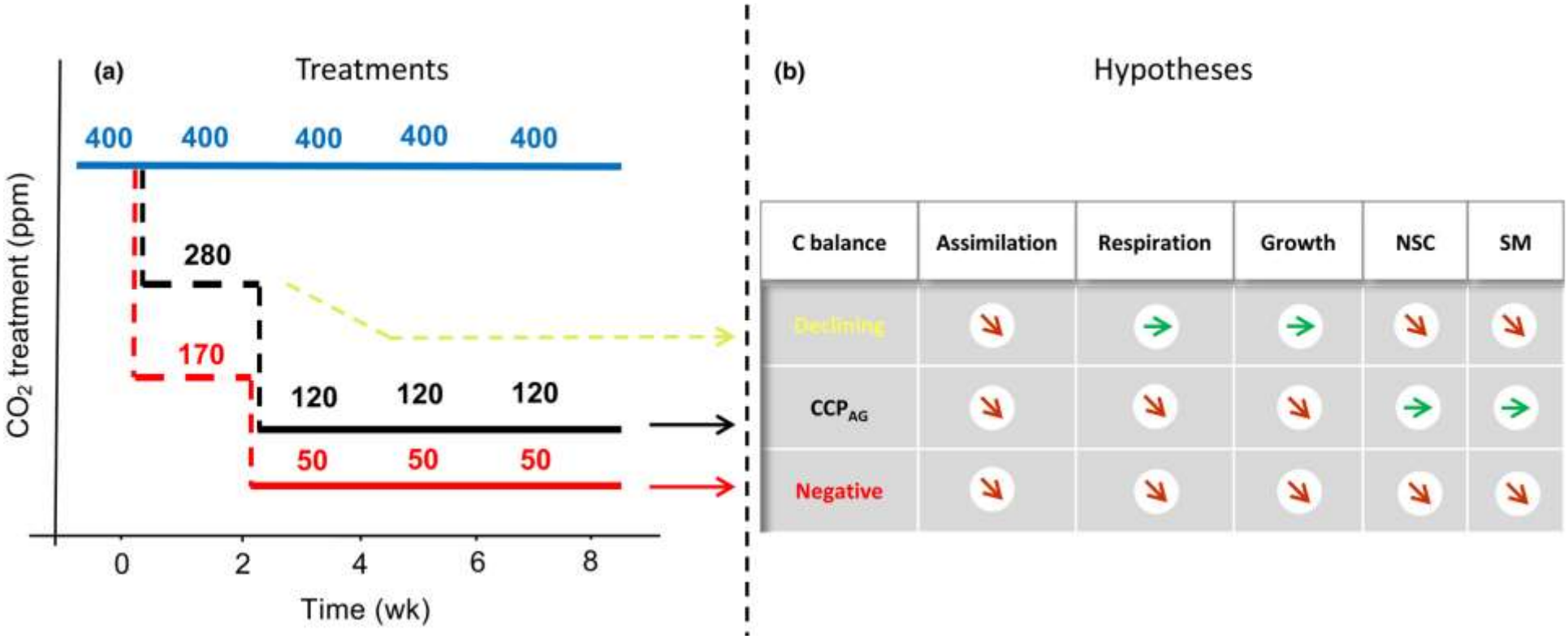

Figure 1. (a) Atmospheric CO_2 concentration ([CO_2], ppm) applied over time and (b) the predicted carbon (C) allocation trade-offs in *Picea abies* along a gradient of C availability. The treatments are shown in (a): blue line indicates 400 ppm [CO_2], maintained throughout the experiment; black line indicates reducing [CO_2] from 400 to 280 ppm, maintained for 2 wk (dashed line), then further to 120 ppm, maintained for 6 wk; red line indicates reducing [CO_2] from 400 to 170 ppm, maintained for 2 wk (dashed line), and then further to 50 ppm, maintained for 6 wk. The predicted C balance and allocation are shown in (b): yellow dashed arrow indicates low CO_2 treatments that lead to declining C availability but C balance still maintains positive, whereas the black arrow and red arrow indicate treatments that result in aboveground C compensation point (CCP_{AG}) and negative C balance, respectively; at positive C balance but limited C supply, nonstructural carbohydrates (NSC) are used to fuel growth and respiration; at CCP_{AG}, allocation to NSC and secondary metabolites (SM) are maintained at the expense of growth and respiration in order to ensure future survival; under negative C balance, all sink activities decrease, but NSC cannot be completely depleted as they are required for osmoregulation, and SM remobilization is limited due to a lack of catabolic enzymes or limited enzymatic access. All hypothesized changes are relative to the control treatment, that is, 400 ppm [CO_2].

(1) under 280 and 170 ppm [CO_2], spruce trees use accumulated NSC storage for growth and respiration whilst still having positive C balance; (2) as [CO_2] decreases and reaches a C compensation point, NSC and SM are reserved at the expense of growth and respiration, particularly in young developing leaves; (3) reducing [CO_2] to 50 ppm causes a negative C balance and thereby decreases all sink activities.

Materials and Methods

Plant material

Norway spruce clones (S21K04200232, Sweden) were initially grown in pots with soil and placed outdoors. In June 2015, one year prior to the experiment, ca. 7-year-old seedlings were pruned to fit in growth chambers and transplanted into pots filled with sand (*i.e.* carbon-free substrate not interfering with measurements of the C balance) and a slow-releasing inorganic fertilizer (Osmocote Start, Everris International B.V., Netherlands).

Growth chambers and [CO_2] manipulation

The study was carried out during summer 2016. Manipulation of atmospheric [CO_2] was achieved by twelve glass chambers coupled to a system allowing scrubbing ambient CO_2 from air and re-adding CO_2 from a gas tank. The facility had been previously built in the greenhouse of the Max Planck Institute for Biogeochemistry in Jena (see Hartmann *et al.*, 2013 for more details). Importantly, the CO_2 re-added to the CO_2-free air had a $\delta^{13}C$ of -38‰, while the outside air in which plants were grown before the experiment had $\delta^{13}C$ of approximately -9‰. Thus all C fixed by the plants under different [CO_2] manipulations received a continuous label that could be traced through plant C metabolism. One spruce sapling was placed into every glass chamber, with roots grown in an airtight pot separated from the aboveground compartment. Supplemental greenhouse lamps were provided during the early morning and later afternoon, and purposely adjusted to avoid high temperature stress during hot days and recovery period (2-3 days after root sampling). Light intensity was measured inside the glass chamber between 5 a.m. and 9 p.m., with overall means of 6.16 ± 0.72 mol m^{-2} d^{-1}, similar to previous experiments (Hartmann *et al.*, 2013; Huang *et al.*, 2017a). Twelve chambers were

divided into three [CO_2] treatments thus yielding four replicates for each of the three treatments, as shown in Fig. **1a**.

Whole-plant gas exchange measurement

Aboveground and belowground CO_2 exchange were measured with Picarro ® cavity ring-down spectrometers, 2131-i and 2101-i, respectively (see Hartmann *et al.*, 2013 for more details). C flux during hour *i* was assumed to be constant within the 2 h cycle and therefore calculated using the following equation:

$$\text{C flux}(\text{mg h}^{-1}) = ([\text{CO}_2]_{\text{in}} - [\text{CO}_2]_{\text{out}})(\mu\text{mol mol}^{-1}) \times \frac{\text{VFR}(\text{l min}^{-1}) \times 60\ (\text{min h}^{-1}) \times 12\ (\text{g mol}^{-1})}{22.4\ (\text{l mol}^{-1})} \times 10^{-3} \qquad \text{Eqn 1}$$

where $[CO_2]_{in}$ and $[CO_2]_{out}$ are the [CO_2] of air entering and exiting the chambers, respectively; VFR is volumetric flow rate of air passing through the chamber (ca. 22 l min^{-1} for aboveground glass chamber, and ca. 3 l min^{-1} belowground pots); 22.4 l mol^{-1} is the molar volume of gas under normal conditions. We then compute daytime assimilation, nighttime respiration and belowground respiration according to the duration over which each occurred (16, 8 and 24 hours, respectively).

Stem diameter and growth measurement

The basal stem diameter variation of each tree (precision 0.8 µm) was monitored continuously with a custom-made dendrometer, averaged every 10 min and recorded with a data-logger (CR23X, Campbell, U.K.). Each pot with the corresponding sapling was placed on a balance (PCB 10000-1, KERN & SOHN GmbH, Germany) inside the growth chamber for continuously measuring the weight. To minimize noise during weighing from watering, a specific watering system was developed: the lower ca. 2 cm of sand were constantly immersed into water thereby wetting the upper layers of sand by capillary action. Water was constantly supplied from a separate reservoir of which the water level was kept constant using a sensor-activated valve.

Relative growth rate (RGR) of total tree fresh biomass at time *i* was calculated based on the initial fresh biomass at time 0 and the fresh biomass at each harvest using equation:

$$\mathrm{RGR}_i = \frac{\log(M_i/M_0)}{t_i - t_0} \qquad \text{Eqn 2}$$

where *Mi* represent fresh biomass of the tree at time *ti* (Hunt, 1982).

Sampling and biomass processing

Sampling was carried out once every two weeks between 14 p.m. and 21 p.m. Approximately 10−15 g of young and old aboveground organs (needles + branches) were sampled using a sharp branch cutter, immediately weighed and then frozen in liquid nitrogen. Fine roots were sampled using scissors, washed and dried before freezing in liquid nitrogen. All fresh tissues were transferred and stored in a freezer (–80 °C) until further processing. Prior to metabolite analysis, fresh needles and branches were separated and homogenized in liquid nitrogen in a mortar. Part of the samples was weighed, freeze-dried and weighed again for determination of the relative water content. Freeze-dried tissues were then ground to fine powder using a ball mill (Retsch® MM400, Haan, Germany) and stored at –20 °C until analysis of soluble sugars, starch and phenolic compounds. The other samples were ground with liquid nitrogen using a mortar and pestle, and stored at –80 °C until analysis of monoterpenes. At the end of the experiment, all trees were destructively harvested for determination of dry biomass of each organ (leaves, branches and roots). From week 8 onward, we observed that all old needles and most young needles exposed to 50 ppm [CO_2] withered and began to fall, all fine roots had died and this resulted in ca. 90% reduction in whole-plant aboveground transpiration compared to 400 and 120 ppm [CO_2].

Soluble sugars and starch analysis

Soluble sugars (glucose, sucrose and fructose) were extracted from freeze-dried samples with distilled water at 65 °C and determined with High-Performance Liquid Chromatography-Pulsed Amperometric Detection (HPLC-PAD), as described by Hartmann *et al.* (2013). For starch determination, the pellet from soluble sugar extraction was digested with a-amylase and

amyloglucosidase (Sigma-Aldrich), followed by glucose determination with HPLC-PAD (S. Landhaeusser, unpublished).

Phenolic compounds analysis

Phenolic compounds were extracted from 30 mg freeze-dried samples in methanol containing 20 µg ml^{-1} of apigenin-7-glucoside (Carl Roth GmbH, Germany) as an internal standard (see Huang *et al.* (2017a) for extraction procedures), and then analyzed with a HPLC coupled to a tandem mass spectrometer as previously described (Hammerbacher *et al.*, 2014). Catechin, gallocatechin, proanthocyanidin B1, astringin and isorhapontin were identified by comparison of retention time and mass spectra with standards, and then quantified using the experimentally determined response factors relative to internal standard (Supporting Information Table **S1**). The sum of these compounds was reported as phenolic compounds. Note that quantification of phenolic compounds was restricted to the availability of standards (Hammerbacher *et al.*, 2014).

Monoterpene analysis

Approximately 100 mg of fresh samples was extracted with 1 ml tert-Butyl methyl ether (TBME) containing 30 µg ml^{-1} 1,9-decadiene (Sigma-Aldrich) as an internal standard. The extraction followed the same procedure used for phenolic compounds, but the supernatant was dehydrated by filtering through a Pasteur pipette filled with glass wool and anhydrous $MgSO_4$. Monoterpenes were identified by Gas Chromatography-Mass Spectrometry (GC-MS) and quantified with Gas chromatography-Flame Ionization Detector (GC-FID), as previously described by Martin *et al.* (2002) with slight modifications. α-pinene, camphene, β-pinene, myrcene, limonene, 1, 8-cineole, bornyl acetate were identified by comparison of mass spectra with of the standards or reference spectra of data bases (Wiley 275, NIST 98, Adams 2205), and quantified with relative response factors (Supporting Information Table **S1**) estimated based on the effective C number concept (Scanlon & Willis, 1985). The sum of these compounds was reported as monoterpenes.

Volatiles collection, identification and quantification

Before tissue sampling (10 a.m. to 14 p.m.), we collected biogenic volatile organic compounds (BVOC) of the air entering and exiting the chambers by using adsorbent tubes filled with 5mm Quarz Wool, Tenax TA 35/60, Carbograph 5TD 40/60 (Markes Environmental, USA). The collection was operated at a flow rate of 215 ml min^{-1} for 30 minutes achieved by using an air sampler (SG350ex, GSA GmbH & CO KG, Germany). The BVOC were analyzed by a thermal desorption-GC-MS consisting of a thermo desorption unit (MARKES, Llantrisant, UK) equipped with an auto-sampler (MARKES, Ultra 50/50). For details of conditions, please see Supporting Information Method **S1**. The major BVOC including α-pinene, β-pinene, 1, 8-cineole and linalool were identified by comparison of retention time and mass spectra with standards (Sigma Aldrich), and then quantified using the external calibration curves. δ-3-carene was quantified using the calibration curve of β-pinene due to lack of standard.

$\delta^{13}C$ of biomass, water-soluble C and phenolic compounds

Approximately 0.1 mg of freeze-dried samples was weighed into tin cups and analyzed with an isotope-ratio-MS (ThermoFinnigan GmbH, Germany). For $\delta^{13}C$ of water soluble C, an aliquot of hot water extract was pipetted into a tin cup and dried at 40°C. The procedure was repeated successively to achieve 0.1 mg dry samples, which were analysed for $\delta^{13}C$ as before. Solid phase extraction (SPE) was used to separate phenolic compounds from other compounds (e.g. sugars, lipids, internal standard) in the methanol extacts. Briefly, 0.5 ml methanol extact was diluted with 4.5 ml distilled water. The 5 ml mixture was then loaded onto a column (Chromabond HR-X, 45 µm, 1 ml/30 mg, Macherey-Nagel Gmbh, Germany) that was pre-conditioned by 1 ml methanol followd by 1 ml water. The column was then sequentially eluted by a gradient of methanol/water solution (v/v) from 10% to 100%. Solutions were collected and analyzed with a LC-MS (Esquire 6000 ESI, Bruker Daltronics, Bremen, Germany). All sugars were washed out by 1 ml 20% methanol/water solution, while phenolic compounds such as catechin and gallocatechin were mainly dissolved by 35% methanol/water solution. Hence, an aliquot of 35% methanol/water elution was pipetted into a tin cup, dried at 40°C and analysed for $\delta^{13}C$ as before. All $\delta^{13}C$ values were reported relative to the international Vienna Pee Dee Belemnite (VPDB), and calculated using equation:

$$\delta^{13}\mathrm{C}(‰) = \left[\frac{\left[\frac{^{13}\mathrm{C}}{^{12}\mathrm{C}}\right]_{sample}}{\left[\frac{^{13}\mathrm{C}}{^{12}\mathrm{C}}\right]_{VPDB}} - 1 \right] * 1000 \qquad \text{Eqn. 3}$$

The precision of the measurement was <0.1‰ based on the lab standard (caffeic acid: –40.46‰). While water-soluble C may contain C from soluble sugars, amino acids and organic acids, it has been demonstrated that water-soluble C is an reliable proxy for the δ^{13}C value of soluble sugars in needles of *Pinus sylvestris* (Brandes *et al.*, 2006).

Data analysis

Each growth chamber was treated as a biological replicate (n=4). All data were checked for normality and homogeneity of variances with Shapiro–Wilk test and Levene tests, respectively, and were log-transformed to meet normality and homoscedasticity as needed. Tukey's honest significance test (HSD, p<0.05) was used to test significant differences between treatments. When values are negative and cannot be log-transformed (e.g., assimilation, stem diameter variation at 50 ppm [CO_2] and δ^{13}C values), we used Wilcoxon's rank-sum test to test significant differences between treatments. To assess the significant differences in temporal trends of NSC and SM concentrations and isotope data, we used repeated-measures ANOVA after checking normality and sphericity with Shapiro–Wilk test and Mauchly's test, respectively. Friedman test was used when assumption of normality or sphercity was violated. For data expressed as the percentage of control (400 ppm [CO_2]), coefficient of variation (*i.e.* relative standard error) was calculated for control treatment, and standard errors of lower [CO_2] treatments were propagated according to error propagation rules. All statistical analysis was conducted in R (version 3.3.2, R Development Core Team, 2016).

Results

Whole-plant gas exchange

Net assimilation declined rapidly right after reducing [CO_2] from 400 ppm to 280 and 170 ppm, whereas both aboveground and belowground respiration were not significantly affected (Fig. **2a,b,d**). From week 2 onwards, net assimilation at 400 ppm decreased from ca. 600 to 300 mg C

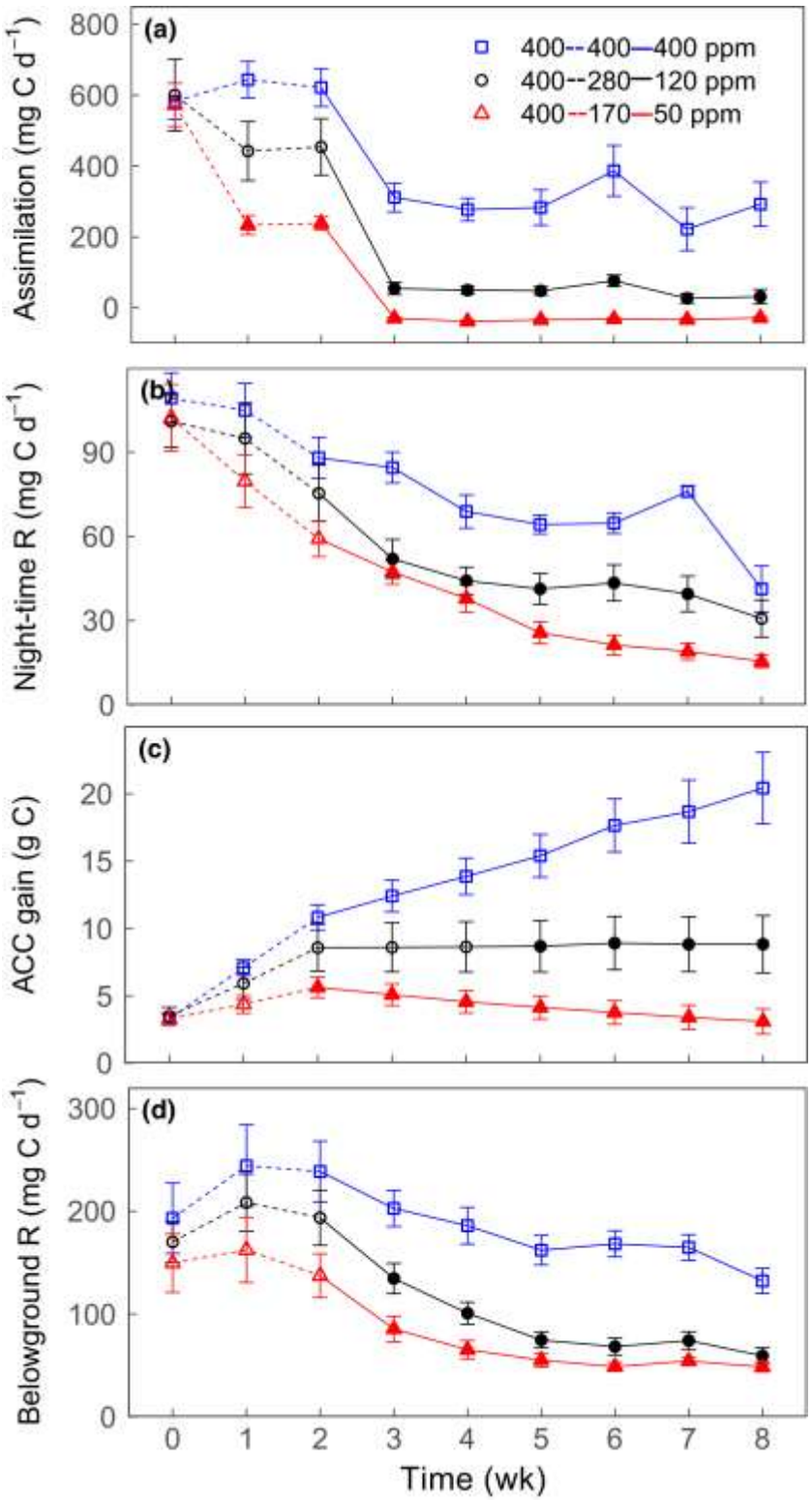

Figure 2. Weekly aboveground (a) net carbon (C) assimilation (mg C d^{-1}), (b) night-time respiration (R; mg C d^{-1}), (c) aboveground accumulative C gain (ACC gain; g C); and (d) belowground respiration (mg C d^{-1}) in *Picea abies* for several different atmospheric CO_2 concentration ($[CO_2]$) treatments: 400 ppm $[CO_2]$ (squares, blue lines); 400–280–120 ppm $[CO_2]$ (circles, black line); 400–170–50 ppm $[CO_2]$ (triangles, red lines). The black and red dashed lines indicate reducing $[CO_2]$ from 400 to 280 ppm and from 400 to 170 ppm, respectively, maintained for 2 wk; the black and red solid lines indicate a further reduction from 280 to 120 ppm and from 170 to 50 ppm, respectively, maintained for 6 wk. Values are the means (mg C) of four individual chambers; error bars represent ± SE. Significant differences between the two lower $[CO_2]$ treatments and ambient $[CO_2]$ (400 ppm) are indicated by closed symbols ($P < 0.05$, Tukey's HSD or Wilcoxon's rank-sum test).

per day possibly due to greenhouse light limitation. However, net assimilation declined to less than 100 mg at 120 ppm and dropped to negative values at 50 ppm [CO_2] (i.e. daytime respiration exceeded gross assimilation; Fig. **2a**). Similarly, respiration was significantly lower at 120 ppm than at 400 ppm ($P<0.05$), but the decrease was proportionally more belowground (ca. 60 %) than aboveground (ca. 40 %) relative to 400 ppm (Fig. **2b,d**). At 120 ppm, respiration was roughly equal to assimilation aboveground, leading to zero C gain after week 2, which we define as aboveground C compensation point (CCP_{AG}; Fig. **2c**). A further [CO_2] reduction from 120 to 50 ppm reduced aboveground respiration, but had less effect on belowground respiration (Fig. **2b,d**) and let to overall C loss (Fig. **2c**).

Growth

During the first two weeks, stem diameter increased at 400 ppm but not at 280 and 170 ppm. From week 2 onwards, stem diameter remained relatively constant at 400 ppm, but showed a significant decline at 120 ppm and decreased even further at 50 ppm (Fig. **3a**). By contrast, fresh biomass increments showed little difference between 400, 280 and 170 ppm during the first two weeks. After week 2, while biomass increased over time at 400 ppm, it remained relatively constant at 120 and 50 ppm, which were similar to each other (Fig. **3b**).

Soluble sugars and starch

After reducing [CO_2] from 400 to 280 and 170 ppm for two weeks, soluble sugars declined by ca. 0- 30% in aboveground organs, and by ca. 40% in roots (Fig. **4a-c)**. A rather rapid decline was observed at week 4 in aboveground organs after reducing [CO_2] from 280 and 170 to 120 and 50 ppm, respectively; after which there were no further reductions in young needles and branches ($P>0.05$, repeated measures ANOVA or Friedman test; Fig. **4a,b**). Similar effects were also observed in old organs (Supporting Information Fig. **S1**). By contrast, reducing [CO_2] to 50 ppm caused a significant decline in root soluble sugars towards the end of the experiment ($P<0.05$, repeated-measures ANOVA; Fig. **4c**). Note that at 50 ppm, concentrations of soluble sugars declined to between 10 − 20 mg g^{-1} in aboveground organs but to almost zero in roots (Supporting Information Fig. **S2**).

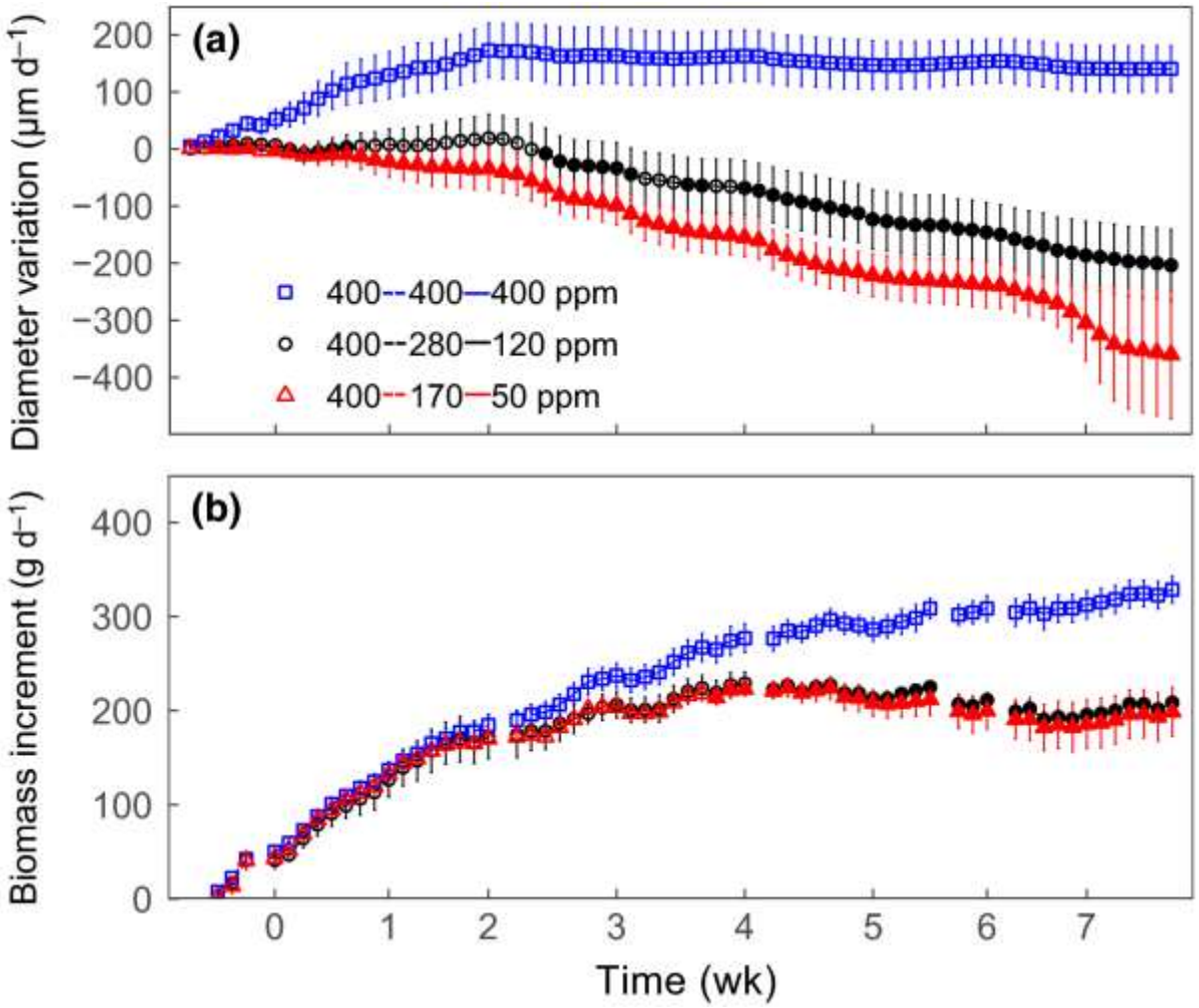

Figure 3. Daily (a) stem diameter variation (µm d^{-1}) and (b) biomass increment (g d^{-1}) in *Picea abies* for the different atmospheric CO_2 concentration ($[CO_2]$) treatments: 400 ppm $[CO_2]$ (squares); 400–280–120 ppm $[CO_2]$ (circles); 400–170–50 ppm $[CO_2]$ (triangles). Values are the means of four individual chambers; error bars represent ± SE. Significant differences between the two lower $[CO_2]$ treatments and ambient $[CO_2]$ (400 ppm) are indicated by closed symbols ($P < 0.05$, Tukey's HSD or Wilcoxon's rank-sum test).

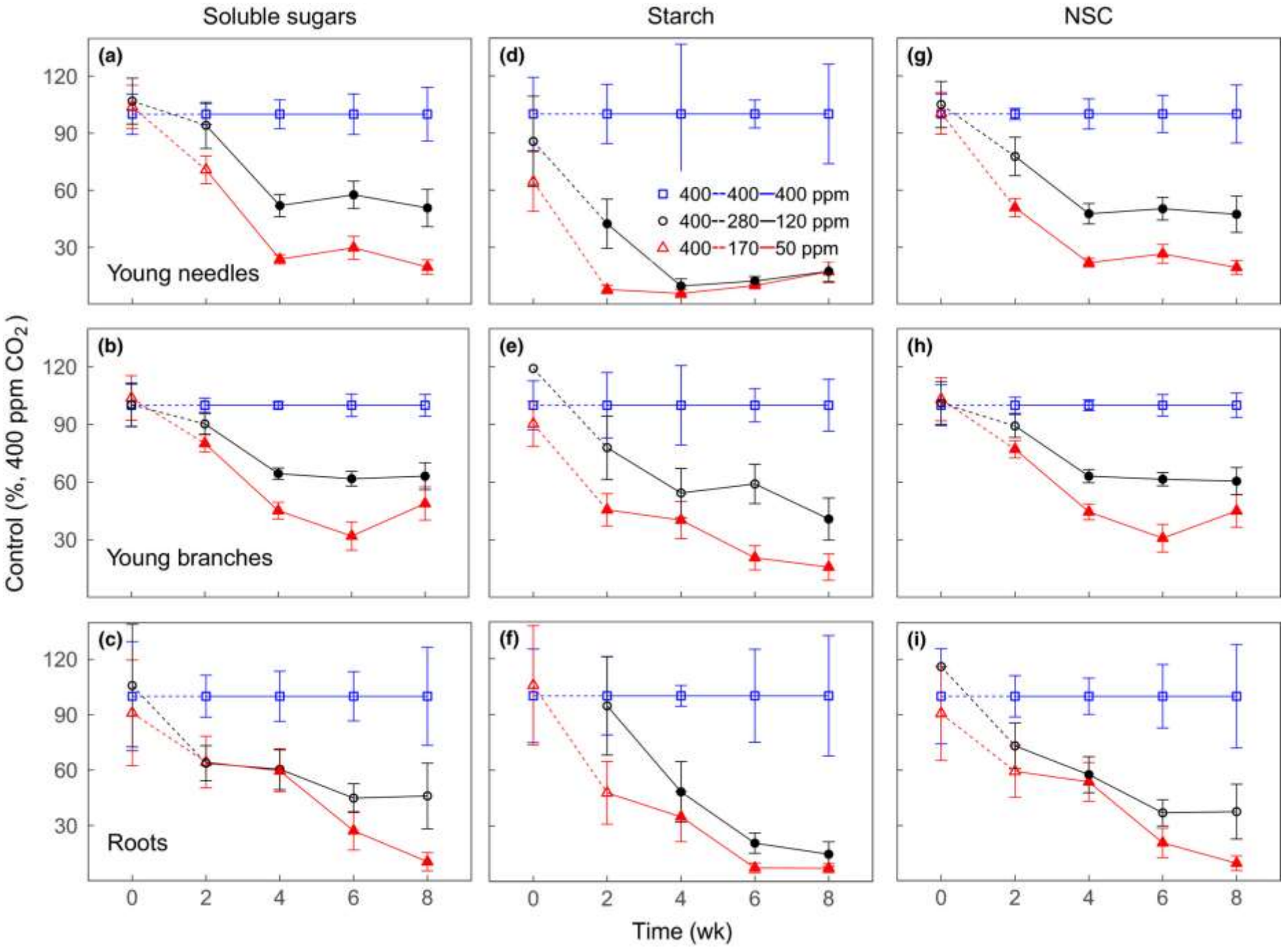
Soluble sugars
Starch
NSC
(a)
(b)
(c)
(d)
(e)
(f)
(g)
(h)
(i)
Young needles
Young branches
Roots
400--400—400 ppm
400--280—120 ppm
400--170—50 ppm
Control (%, 400 ppm CO2)
Time (wk)
120
90
60
30
0
2
4
6
8

Figure 4. Concentrations of (a–c) soluble sugars, (d–f) starch and (g–i) total nonstructural carbohydrates (NSC; soluble sugars + starch) of young needles, young branches and roots in *Picea abies* for the different atmospheric CO_2 concentration ($[CO_2]$) treatments: 400 ppm $[CO_2]$ (squares, blue line); 400–280–120 ppm $[CO_2]$ (circles, black line); 400–170–50 ppm $[CO_2]$ (triangles, red line), expressed as a percentage of control (400 ppm $[CO_2]$). The black and red dashed lines indicate reducing $[CO_2]$ from 400 to 280 ppm and from 400 to 170 ppm, respectively, maintained for 2 wk; the black and red solid lines indicate a further reduction from 280 to 120 ppm and from 170 to 50 ppm, respectively, maintained for 6 wk. Error bars at 400 ppm $[CO_2]$ represent coefficient of variation (i.e. relative SE). Error bars at 280, 170, 120 and 50 ppm $[CO_2]$ represent propagated SE. Significant differences between the two lower $[CO_2]$ treatments and ambient $[CO_2]$ (400 ppm) are calculated based on the raw concentrations, and indicated by closed symbols ($P < 0.05$, Tukey's HSD).

Reducing [CO_2] from 400 to 280 and 170 ppm caused a stronger decline in aboveground starch than in soluble sugars at week 2 (Fig. **4d,e**). Starch levels continuously declined after a further reduction from 280 and 170 ppm to 120 and 50 ppm, respectively (Fig. **4d-f**); at week 8, starch concentrations in all organs declined to almost zero at 120 and 50 ppm (Supporting Information Fig. **S2**). Because concentrations of starch were much lower than of soluble sugars across organs and treatments (Supporting Information Fig. **S2**), responses of total NSC (soluble sugars + starch; Fig. **4g-i**) concentrations were similar to those of soluble sugars.

Phenolic compounds and monoterpenes

The response of phenolic compounds and monoterpenes to low [CO_2] (expressed as a percentage of control, 400 ppm [CO_2]) differed among organs (Fig. **5**). Reducing [CO_2] from 400 to 280 and 170 ppm had no effects on phenolic compounds by week 2 in all organs except in young branches where there was a decline at 170 ppm (Fig. **5a-c**). A further reduction to 120 ppm at week 2 slightly decreased aboveground concentrations of phenolic compounds, but not significant relative to 400 ppm ($P>0.05$; Fig. **5a,b**). However, reducing [CO_2] to 50 ppm eventually strongly decreased phenolic compounds at week 8, by 85% and 50% in young needles and young branches, respectively, relative to 400 ppm; by contrast, there were no differences in old branches except a significant increase at week 4 (Supporting Information Fig. **S3**). Under 50 ppm [CO_2], root concentrations of phenolic compounds significantly decreased over time ($P<0.05$; Friedman test). Note that concentrations of phenolic compounds in young needles declined to almost zero at 50 ppm [CO_2] towards the end of the experiment (Supporting information Fig. **S4**).

Aboveground concentrations of monoterpenes were also similar between 400 and 120 ppm and remained relatively constant over time ($P>0.05$, repeated measures ANOVA or Friedman test; Fig. **5d,e**). However, reducing [CO_2] to 50 ppm resulted in ca. 30-40% decrease in concentrations of monoterpenes relative to 400 ppm, although not statistically significant (Fig. **5d,e**). By contrast, monoterpenes remained relatively constant in old needles and branches (Supporting information Fig. **S3**). Root monoterpenes gradually decreased in both low [CO_2] treatments which did not differ (Fig. **5f**). Concentrations of phenolic compounds were generally

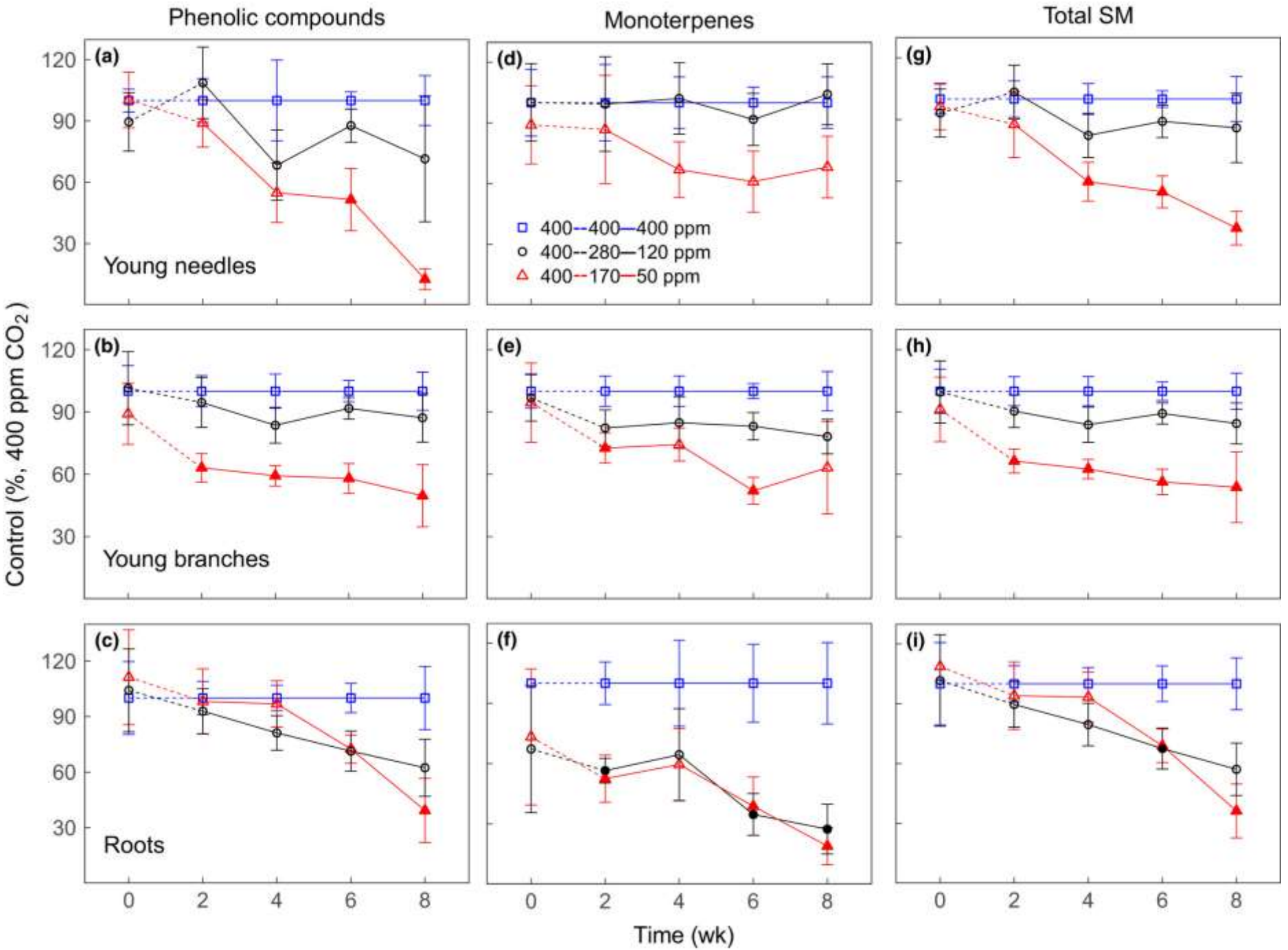
Phenolic compounds
Monoterpenes
Total SM
(a)
(b)
(c)
(d)
(e)
(f)
(g)
(h)
(i)
Young needles
Young branches
Roots
400–400–400 ppm
400–280–120 ppm
400–170–50 ppm
Control (%, 400 ppm CO2)
Time (wk)
120
90
60
30
0
2
4
6
8

Figure 5. Concentrations of (a–c) phenolic compounds, (d–f) monoterpenes and (g–i) total secondary metabolites (SM; phenolic compounds + monoterpenes) of young needles, young branches and roots in *Picea abies* for the different atmospheric CO_2 concentration ([CO_2]) treatments: 400 ppm [CO_2] (squares, blue line); 400–280–120 ppm [CO_2] (circles, black line); 400–170–50 ppm [CO_2] (triangles, red line), expressed as a percentage of control (400 ppm [CO_2]). The black and red dashed lines indicate reducing [CO_2] from 400 to 280 ppm and from 400 to 170 ppm, respectively, maintained for 2 wk; the black and red solid lines indicate a further reduction from 280 to 120 ppm and from 170 to 50 ppm, respectively, maintained for 6 wk. Error bars at 400 ppm [CO_2] represent coefficient of variation (i.e. relative SE). Error bars at 280, 170, 120 and 50 ppm [CO_2] represent propagated SE. Significant differences between the two lower [CO_2] treatments and ambient [CO_2] (400 ppm) are calculated based on the raw concentrations, and indicated by closed symbols ($P < 0.05$, Tukey's HSD).

higher than of monoterpenes across organs (Supporting Information Fig. **S4**), thereby total SM (phenolic compounds + monoterpenes; Fig. **5g-i**) followed similar trends to phenolic compounds.

Unlike for monoterpenes stored in tissues, emissions of volatile monoterpenes exhibited large variations over time (Fig. **6**). After week 2, emissions of α- and β-pinene at 400 and 120 ppm [CO_2] remained relatively constant and only slightly increased at week 8, but there was a much stronger increase at 50 ppm [CO_2] by week 8, although not statistically significant compared to 400 ppm [CO_2] (Fig. **6a,b**). By contrast, linalool emissions declined to almost zero at 50 ppm [CO_2], which were significantly lower than 400 ppm [CO_2] at week 6 and 8 ($P<0.05$; Fig. **6e**). There were no clear differences in emissions of δ−3−carene, 1,8−cineole (Fig. **6c,d**). The contrasting emissions of pinenes versus linalool to 50 ppm [CO_2], resulted in no differences in total emissions of summed monoterpenes across [CO_2] treatments (Fig. **6f**).

Allocation of newly-assimilated C into biomass, water-soluble C and phenolic compounds

Prior to the treatments, the $\delta^{13}C$ of biomass and of water-soluble C were higher than that of phenolic compounds across organs (Fig. **7**). Decreases in $\delta^{13}C$ indicate incorporation of newly-assimilated C. Reducing [CO_2] from 400 to 280 and 170 ppm significantly decreased allocation of newly-assimilated C to biomass (bulk) and water-soluble C at week 2 ($P<0.05$; Fig. **7a-f**). After reducing [CO_2] to 120 ppm at week 2, the $\delta^{13}C$ of biomass and water-soluble C significantly declined over time in aboveground organs ($P<0.05$, repeated measures ANOVA or Friedman test) except for the $\delta^{13}C$ of biomass of young needles (Fig. **7a,b,d,e**), indicating a continuous allocation of newly-assimilated C, but this apparently did not occur in roots (Fig. **7c,f**). At 50 ppm [CO_2], only minor allocation of newly-assimilated was observed in young needles, and $\delta^{13}C$ of water soluble C even showed an increase in young branches and roots (Fig. **7e,f**).

For phenolic compounds, newly-assimilated C was observed at 280 and 170 ppm in young organs, although less than 400 ppm (Fig. **7g,h**); in old organs, however, there was little incorporation of new-assimilated C (Supporting information Fig. **S5**). After a reduction to 120 ppm at week 2, $\delta^{13}C$ of phenolic compounds only slightly declined in young needles, but

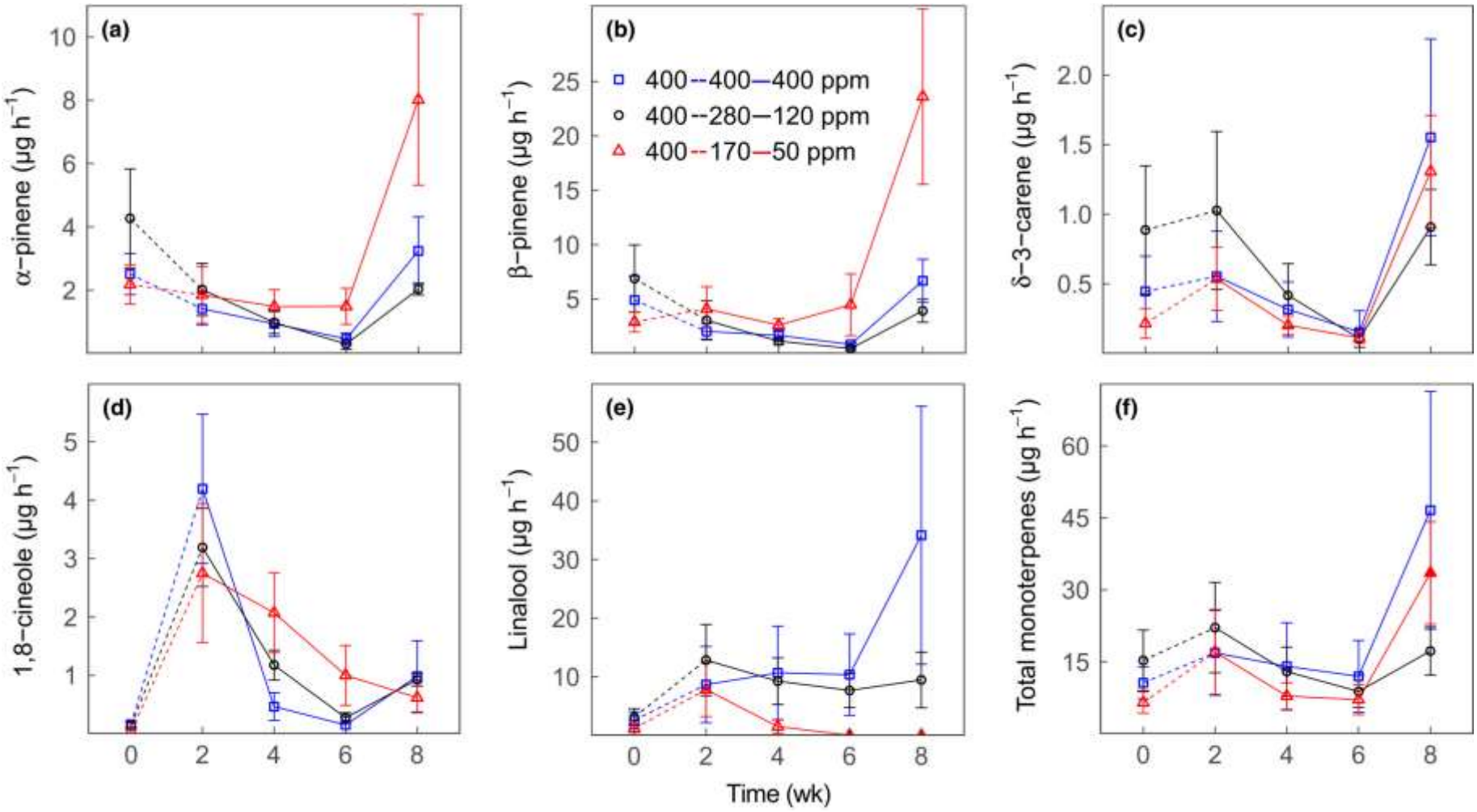

Figure 6. Aboveground emissions (µg h^{-1}) of (a) α-pinene, (b) β-pinene, (c) δ-3-carene, (d) 1,8-cineole, (e) linalool and (f) total monoterpenes in *Picea abies* for the different atmospheric CO_2 concentration ($[CO_2]$) treatments: 400 ppm $[CO_2]$ (squares, blue lines); 400–280–120 ppm $[CO_2]$ (circles, black lines); 400–170–50 ppm $[CO_2]$ (triangles, red lines). The black and red dashed lines indicate reducing $[CO_2]$ from 400 to 280 ppm and from 400 to 170 ppm, respectively, maintained for 2 wk; the black and red solid lines indicate a further reduction from 280 to 120 ppm and from 170 to 50 ppm, respectively, maintained for 6 wk. Values are the means of four individual chambers; error bars represent ± SE. Significant differences between the two lower $[CO_2]$ treatments and ambient $[CO_2]$ (400 ppm) are indicated by close symbols ($P < 0.05$, Tukey's HSD).

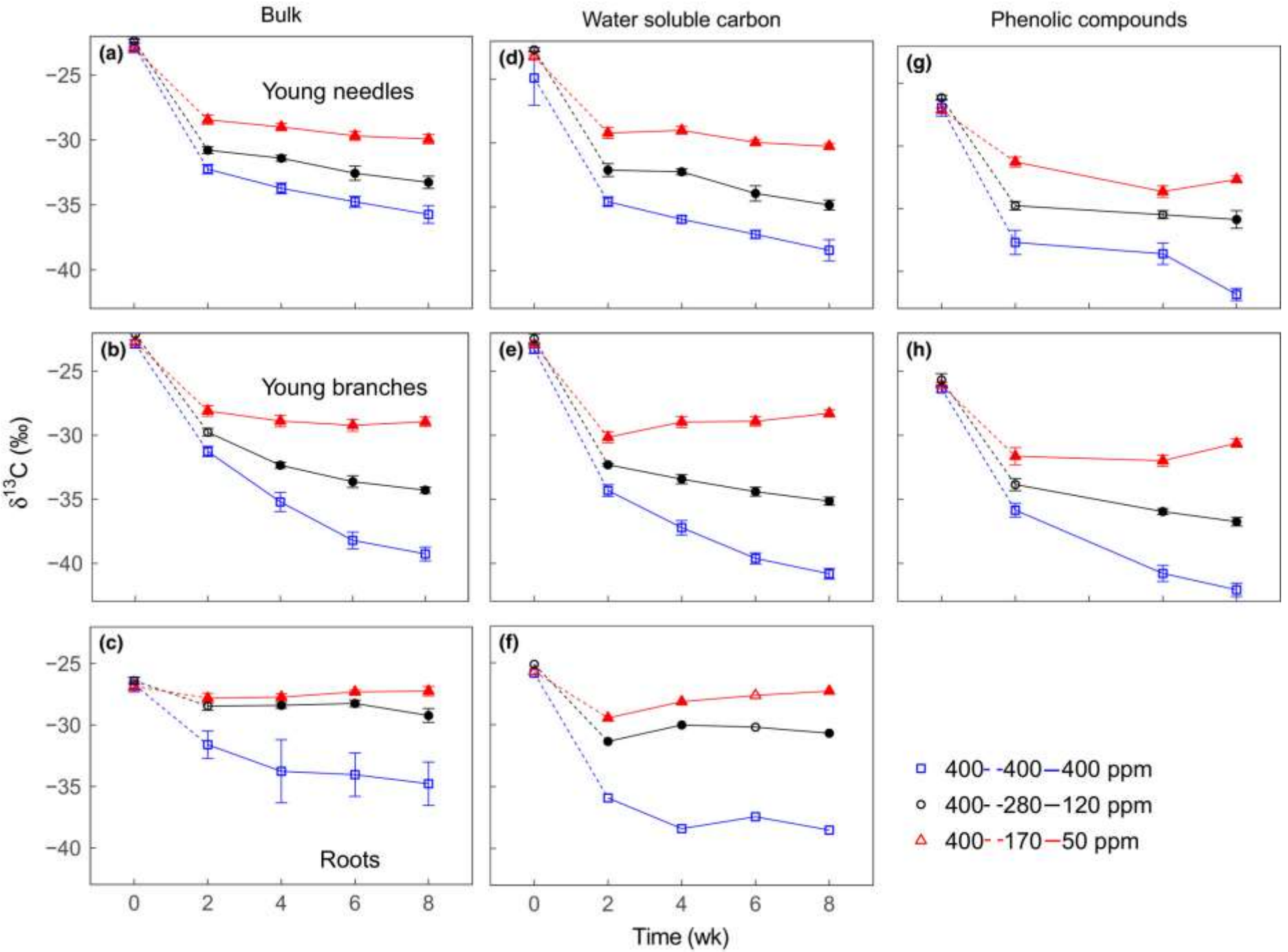
Bulk
Water soluble carbon
Phenolic compounds
(a)
Young needles
(d)
(g)
(b)
Young branches
(e)
(h)
(c)
Roots
(f)
δ13C (‰)
−25
−30
−35
−40
0
2
4
6
8
Time (wk)
400- -400—400 ppm
400- -280—120 ppm
400- -170—50 ppm

Figure 7. $\delta^{13}C$ (‰) of (a–c) bulk tissue, (d–f) water soluble carbon and (g–i) phenolic compounds in *Picea abies* for the different atmospheric CO_2 concentration ($[CO_2]$) treatments: 400 ppm $[CO_2]$ (squares, blue lines); 400–280–120 ppm $[CO_2]$ (circles, black lines); 400–170–50 ppm $[CO_2]$ (triangles, red lines). The black and red dashed lines indicate reducing $[CO_2]$ from 400 to 280 ppm and from 400 to 170 ppm, respectively, maintained for 2 wk; the black and red solid lines indicate a further reduction from 280 to 120 ppm and from 170 to 50 ppm, respectively, maintained for 6 wk. Values are the means of four individual chambers; error bars represent ± SE. Significant differences between the two lower $[CO_2]$ treatments and ambient $[CO_2]$ (400 ppm) are indicated by closed symbols ($P < 0.05$, Tukey's HSD or Wilcoxon's rank-sum test).

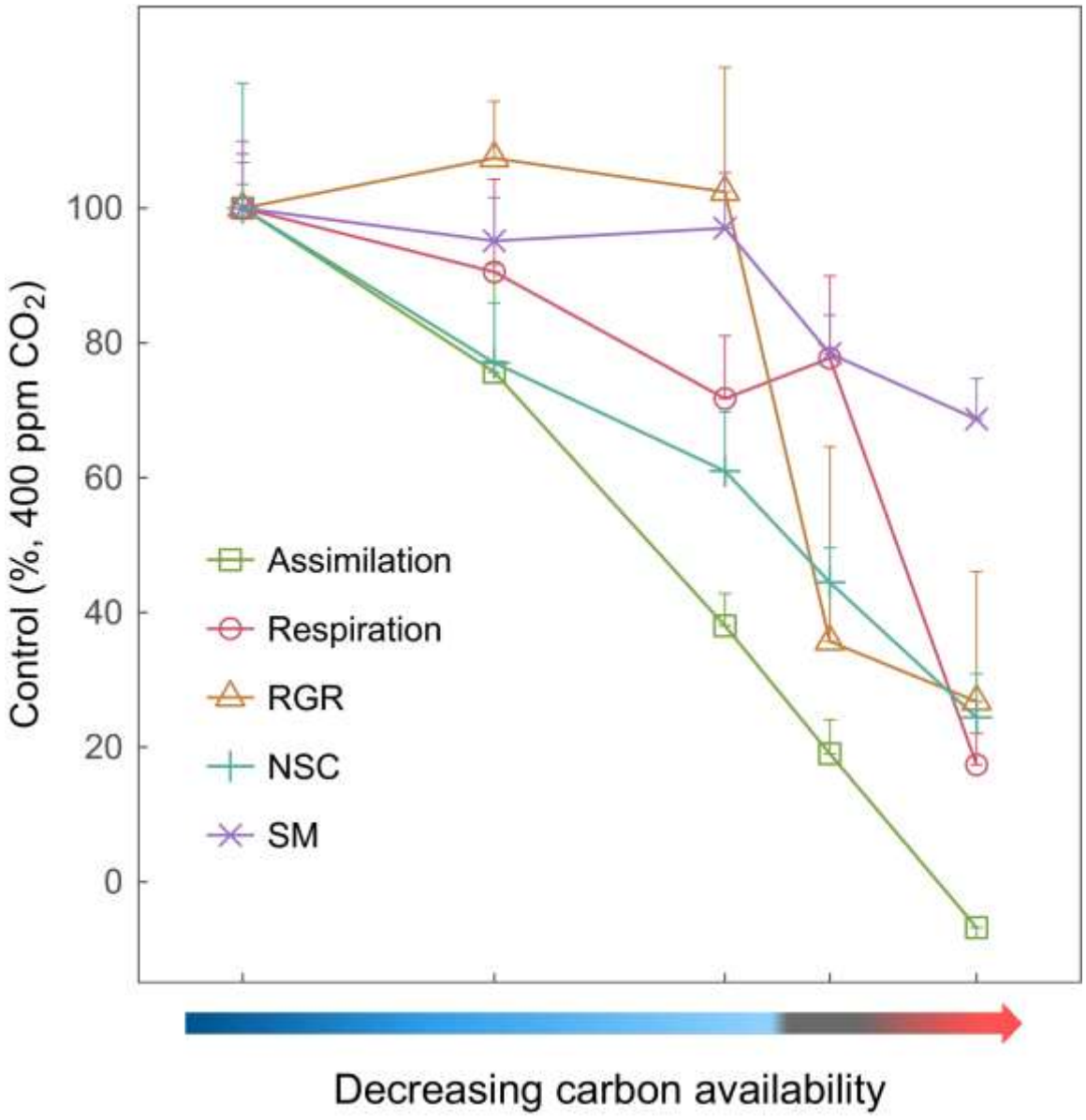

Figure 8. Trade-offs between aboveground daytime net assimilation (squares, green line) and night-time respiration (circles, pink line), whole-tree relative growth rate (RGR, triangles, brown line), and weighted nonstructural carbohydrates (NSC; plus symbol, blue line) and secondary metabolites (SM; cross symbol, violet line) in *Picea abies* along a gradient of carbon (C) availability, expressed as a percentage of control (400 ppm atmospheric CO_2 concentration ($[CO_2]$)). The arrow below the *x*-axis indicates decreasing gradients of C availability, spanning from positive C balance (blue; 400, 280, 170 ppm $[CO_2]$) to the aboveground C compensation point (black; 120 ppm $[CO_2]$) and then to a negative C balance (red; 50 ppm $[CO_2]$). Whole-aboveground daytime assimilation and nighttime respiration were averaged over the last 2 d before organ sampling. Whole-tree RGR was calculated using intervals between Weeks 0 and 2, and between Weeks 2 and 6. NSC and SM concentrations were weighted by multiplying concentrations in needles, branches (averaged from young and old organs) and roots with the relative contribution of dry biomass of each organ (needles, branches and roots) that was assessed at the end of the experiment and accounting the biomass loss of organs from each sampling. The dry biomass ratio between needles, branches and roots was assumed to be constant after Week 2, as most growth occurred during the first 2 wk. Values are the means of three or four chambers; error bars at 400 ppm $[CO_2]$ represent coefficient of variation (i.e. relative SE, n = 3 or 4). Error bars at 280, 170, 120 and 50 ppm represent propagated SE.

significantly declined over time in young branches ($P<0.05$, repeated measures ANOVA; Fig. **7h**), suggesting a continuous allocation of newly-assimilated C. After a reduction from 170 to 50 ppm [CO_2], $\delta^{13}C$ of phenolic compounds slightly increased in young branches by week 8 (Fig. **7h**). By contrast, $\delta^{13}C$ of phenolic compounds remained relatively constant in old branches, irrespective of [CO_2] treatments ($P>0.05$, Friedman test; Supporting information Fig. **S5**).

After reducing [CO_2] from 400 to 280 and 170 ppm, assimilation strongly decreased but C balance still maintained positive; NSC decreased faster than respiration and RGR, but SM remained relatively constant (Fig. **8**). A further reduction from 280 to 120 ppm [CO_2] caused aboveground C compensation point, and decreased growth more than NSC and SM. Reducing [CO_2] to 50 ppm led to negative C balance, where activities of all sinks strongly declined except that SM only declined by 20-30% relative to 400 ppm [CO_2] (Fig. **8**).

Discussion

Manipulation of the whole-tree C balance via changing [CO_2], coupled with application of isotopic labelling, allowed us to explore how trees allocate stored/newly-assimilated C for growth, storage and defence under different amounts of C supply. Our treatments were intended to create a situation of declining C availability to force trees into a severe resource trade-off, not necessarily to a new steady state. At CCP_{AG} (120 ppm), whole-plant growth decreased as root NSC reserves continuously declined, whereas aboveground concentrations of soluble sugars initial declined but then remained constant due to a continuous allocation of newly-assimilated C. Soluble sugar levels further decreased under negative C balance (50 ppm), resulting in a complete depletion in roots probably due to impeded transport of newly-assimilated C. By contrast, concentrations of SM (phenolic compounds + monoterpenes) remained relatively constant in young organs until CCP_{AG}, which was also the case in old branches of dying trees below CCP_{AG} at week 8. Above and at CCP_{AG}, newly-assimilated C was continuously allocated to phenolic compounds in young branches, but not in old organs. The emissions of aboveground volatile monoterpenes were unaffected by [CO_2] treatments.

Down-regulation of growth and respiration to maintain soluble sugars for survival

How trees build up NSC pools, *i.e.* accumulation versus reserve formation (Chapin *et al.*, 1990), has been hotly debated in recent years (Sala *et al.*, 2012; Wiley & Helliker, 2012; Dietze *et al.*, 2014; Palacio *et al.*, 2014). Our results showed that moderate C limitation (280 and 170 ppm [CO_2]) resulted in rapid declines in assimilation, leading trees to use NSC storage for maintaining growth and respiration (Fig. **8**). This may indicate that NSC storage is at least partially driven by the balance between C supply and C demand, *i.e.* accumulation (Chapin *et al.*, 1990; Hartmann & Trumbore, 2016). These responses at the whole-tree level are in agreement with results from studies on *Eucalypts* grown at 280 ppm [CO_2], where leaf NSC concentrations decreased (Ayub *et al.*, 2011) but not leaf respiration (Ayub *et al.*, 2011; Ayub *et al.*, 2014) or growth (Ghannoum *et al.*, 2010).

A further reduction to 120 ppm, *i.e.* CCP_{AG}, decreased growth faster than NSC levels (Fig. **8**), as aboveground concentrations of soluble sugars initially declined and then remained constant (Fig. **4**). Soluble sugars were apparently available for metabolism because concentrations further declined when [CO_2] was reduced to 50 ppm, *i.e.* negative C balance. This may indicate that under CCP_{AG}, soluble sugars are preferentially maintained in aboveground organs at the expense of growth. Isotope data further show continuous incorporation of newly-assimilated C into water-soluble C at CCP_{AG}, in particular in young organs (Fig. **7**). This suggests C fluxes in and out of soluble sugar pools were fine-tuned to achieve "operational" levels. Such regulation of soluble sugar pools may represent a safety margin to avoid C exhaustion, and thus can be interpreted as reserve formation that occurred at the expense of growth (Chapin *et al.*, 1990; Hartmann & Trumbore, 2016; Martínez-Vilalta *et al.*, 2016). Similar patterns were also observed at the leaf level in *Arabidopsis* (Gibon *et al.*, 2009). By contrast, starch declined almost to zero at CCP_{AG}, suggesting that soluble sugars were prioritized over starch as long-term storage. Overall, total NSC responses generally support the theoretical model that NSC pools reflect two processes: accumulation that supports growth and reserve formation that ensures future survival at the expense of immediate development.

Reducing C availability to the point where there is no net plant C gain (CCP_{AG}) may affect the sink strength of growth and respiration to different degrees in different organs. These are in

turn reflected in the dynamics of their substrates, the soluble sugars. We found organ-specific response of growth sink strength by tracing the allocation of newly-assimilated C across organs. At CCP_{AG}, spruce invested more newly-assimilated C into growth of aboveground organs than of roots, consistent with the functional equilibrium hypothesis that resources are allocated to organs that are responsible for acquiring the most limiting resource – in this case, CO_2 (Poorter *et al.*, 2012). Those results are in contrast to the study of Hartmann *et al.* (2015), which showed a continuous allocation of newly-assimilated C into roots at 40 ppm [CO_2]. It is likely because allocation priorities vary with phenology. In our study, we exposed spruce trees to low CO_2 treatments between May and July when aboveground growth of above-ground tissues is a strong sink for C, whereas Hartmann *et al.* (2015) applied 40 ppm [CO_2] treatment after growth and lignification of above-ground tissues were completed.

Reducing [CO_2] to CCP_{AG} (120 ppm) constrained respiration more in belowground (~ 60% decline) than aboveground (~ 40% decline) organs compared to plants grown under ambient [CO_2]. This possibly reflects that respiratory demands of aboveground processes (e.g. sucrose synthesis, phloem loading and turnover of photosynthetic proteins) are prioritized over root processes (e.g. ion uptake). Unfortunately, our experimental setup did not allow differentiating root respiration from heterotrophic respiration (*i.e.* microorganisms decomposing root exudates and litter). Given that belowground respiration was similar between roots grown at CCP_{AG} (120 ppm) and roots dying from negative C balance (50 ppm) at week 8, it is likely that belowground respiration in both low [CO_2] treatments were mainly from microorganisms decomposing root litter. This would mean that C limitation on root respiration may have been underestimated in our experiment.

Preferential maintenance of NSC over respiration occurred at 50 ppm when NSC declined from ca. 45% of controls at 120 ppm to ca. 25% at 50 ppm, while respiration declined from ca. 75% of controls at 120 ppm to ca. 20% at 50 ppm (Fig. **8**). This is consistent with the results of Martínez-Vilalta *et al.* (2016), which showed that average minimum NSC (mostly as soluble sugars) across diverse plant species are ca. 36% of seasonal maximums. Such minimums may represent thresholds below which plants cannot survive and, therefore, are tightly regulated.

Even when trees were dying under 50 ppm [CO_2]-induced C starvation, aboveground concentrations of soluble sugars maintained relatively constant over time (Fig. **4**), in agreement with results from starvation treatments induced by shading (Sevanto *et al.*, 2014; Wiley *et al.*, 2017b; Weber *et al.*, 2018) and low [CO_2] (Hartmann *et al.*, 2015). In contrast to aboveground organs, spruce roots completely depleted soluble sugars in the starvation treatment, which may have caused root death from C exhaustion. These results suggest that spruce saplings at CCP_{AG}, i.e. source limitation, prioritize investment of newly-assimilated C into aboveground processes, causing a depletion of locally stored carbohydrates in roots.

Down-regulation of growth under C limitation to maintain defense

Similar to NSC storage, allocation to SM is often thought to be driven by the balance between C assimilated via photosynthesis (source process) and C demand for growth and respiration (sink processes). Our results show that spruce trees continuously invested C into SM (phenolic compounds + monoterpenes) in young organs until CCP_{AG} (120 ppm), resulting in no significant decline in SM relative to control (400 ppm). This occurred at the expense of other sinks (e.g. NSC storage, growth and respiration), suggesting that C was preferentially allocated to SM production. This is contrary to the theoretical predictions of the C-nutrient balance hypothesis (Bryant *et al.*, 1983) and the growth-differentiation balance hypothesis (Herms & Mattson, 1992), and against empirical evidence from induced C starvation by shading (Roberts & Paul, 2006).

In Norway spruce, those phenolic (Hammerbacher *et al.*, 2014; Hammerbacher *et al.*, 2018) and monoterpene compounds (Martin *et al.*, 2002) have been shown to play an important role in defense against biotic attack. In addition, phenolic compounds (Neilson *et al.*, 2013) and volatile monoterpenes (Vickers *et al.*, 2009) are known to have anti-oxidant properties, therefore maybe required for reducing oxidative damage induced by excess electron transport under low [CO_2] (Galvez-Valdivieso *et al.*, 2009). Hence, prioritization of SM over growth and respiration may reflect increased demands for protecting aboveground young organs, which are of great value for assimilation especially under limited C supply, in agreement with the optimal defense hypothesis that organs that are of greater value should be better protected (Tomonori

et al., 2017). However, such allocation patterns were not seen in wheat plants, which produced significantly less phenolic compounds in aboveground organs at 170 than at 400 ppm [CO_2] (Huang *et al.*, 2017a). The contrasting responses indicate that allocation to defence may follow a different strategy in long-lived organisms like trees compared to annual herbaceous plants, as suggested by resource availability hypothesis (Coley *et al.*, 1985). The long lifespan of trees increases the risk to encounter periods of abiotic (*i.e.* drought, heat waves and cold) or biotic stresses (*i.e.* insect attack and pathogen infestation) and a conservative allocation strategy that prioritize SM over growth may therefore ensure long-term survival.

Terpene emissions serve a double role in plants: scavenge reactive oxygen species (Vickers *et al.*, 2009), and defend against herbivores and pathogens (Holopainen & Gershenzon, 2010; Heil, 2014). We observed contrasting emissions of α- and β-pinene versus linalool as [CO_2] decreased. α- and β-pinene emissions increased under negative C balance which may be attributed to the physical release from the loss of old foliage, whereas linalool emissions are likely produced *de novo* and thus declined in trees dying under negative C balance at week 8. Linalool has been shown to be the major terpenoid emitted from methyl jasmonate (MeJA)-treated Norway spruce (Martin *et al.*, 2003), herbivore-attacked mountain birth (*Betula pubescens*) and poplar trees (Eberl *et al.*, 2017). Hence, a decrease in linalool emissions under negative C balance may diminish the ability of Norway spruce to defend against herbivores such bark beetles. Such changes in terpenoids blend provide new perspectives on how abiotic stress such as drought increases susceptibility of spruce trees to bark beetle attack (Ryan *et al.*, 2015).

By using a complete mass-balance approach, we found that decreasing [CO_2] treatments led to a net loss of NSC storage. By contrast, allocation to SM, calculated as changes in SM as a percentage of newly-assimilated C, remained relative constant (ca. 3–5%) across [CO_2] treatments. This also suggests allocation to SM was preferentially maintained at the expense of NSC storage (Supporting Information Table **S2**). However, we underscore here that differences between measurement devices and techniques, as well as the incompleteness of the dataset (stems and tap roots were not assessed, also not root exudation or microbial decomposition of root litter), still prevent an accurate estimation of quantitative partitioning of available C into

different sinks. For example, we did not measure the C allocation in root exudates, which may constitute up to 50% of the daily C assimilation (van Dam & Bouwmeester, 2016).

Our experiment was carried out in the greenhouse, therefore the relative changes in NSC and SM as a percentage of control indicate treatment effects under the given conditions. Extrapolation of those results to field conditions where other environmental factors may come into play, should be carried out with caution. In contrast to the greenhouse, higher light intensities and lower air temperatures in the field along with an elevated risk of herbivory and pathogen attack may impact assimilation, RGR, NSC and SM more under ambient [CO_2] than under low [CO_2] conditions. Consequently, the effects of C limitation on NSC and SM in the greenhouse would likely be exacerbated under field conditions.

Conclusion and outlook

We provided mechanistic evidence for allocation strategies that appear to be consistent with coordination of supply and demand in the long run, and for trade-offs in the allocation of photosynthetic products to growth, storage and defence. We conclude that spruce trees have a conservative allocation strategy where growth and respiration can be down-regulated to maintain 'operational' levels of NSC while investing into future survival by producing SM (Fig. **9**). Moreover, by tracing fluxes of newly-assimilated C, we highlight an optimal allocation strategy: under source limitation, plants prioritize investment of newly-assimilated C to aboveground young tissues even at expense of root death from C exhaustion (Fig. **9**). Such changes in C allocation strategies are important for us to understand and predict how trees respond to environmental changes such as drought (Anderegg *et al.*, 2015; Ryan *et al.*, 2015), shading (Roberts & Paul, 2006), defoliation (Anderegg & Callaway, 2012) and biotic interactions.

Future studies should integrate the allocation strategies uncovered in small trees in highly controlled growth chambers to large trees in field conditions known to have different light quantify and temperature and thus different source-sink relations (McDowell *et al.*, 2013; Poorter *et al.*, 2016). Moreover, active constraints on growth via phytohormonal regulation have been observed under a variety of stresses including drought (Skirycz et al., 2010) and cold (Achard et al., 2008) in *Arabidopsis*, and low [CO_2] in wheat (Huang *et al.*, 2017b). However,

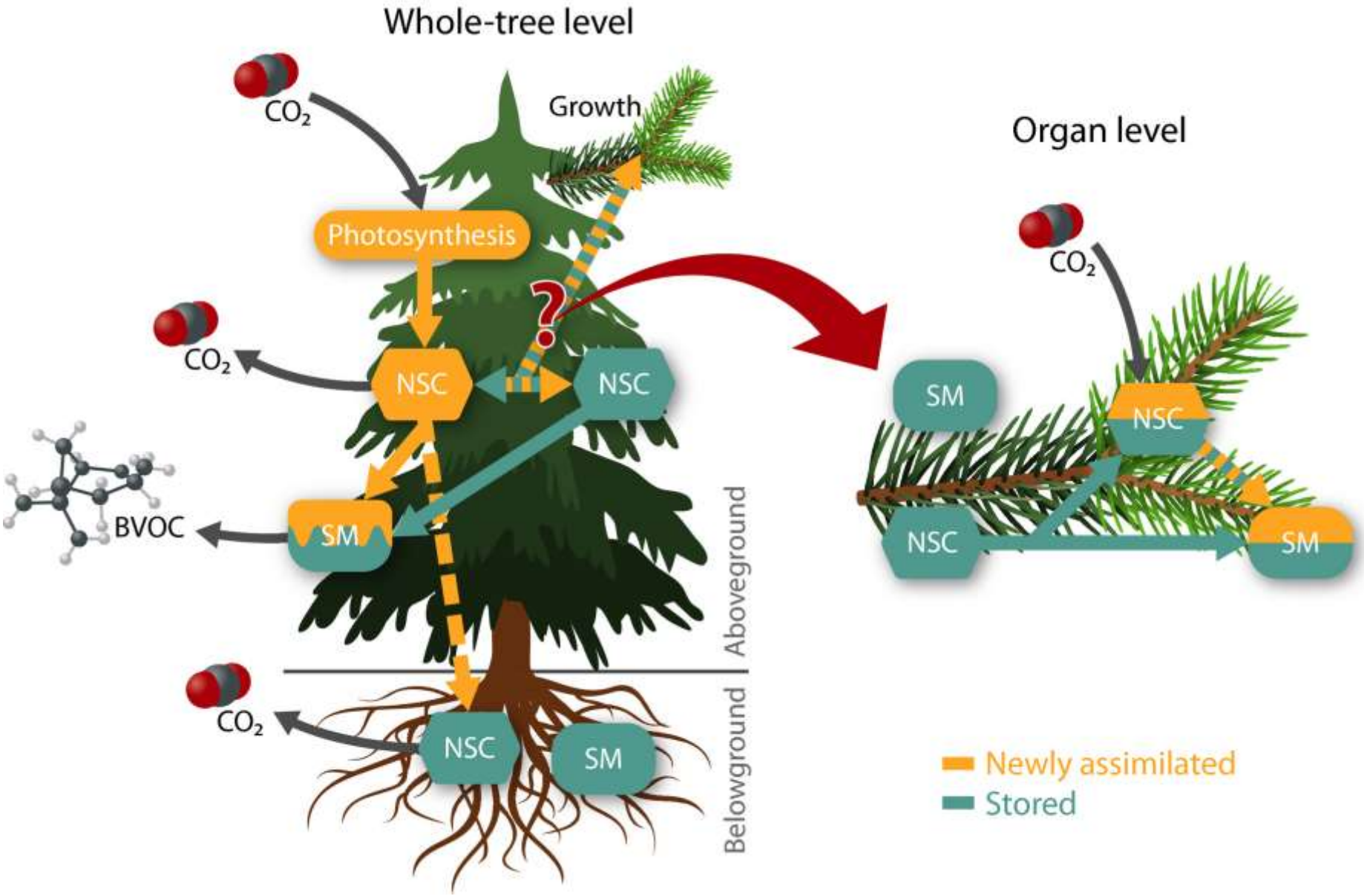
Whole-tree level
CO_2
Growth
Photosynthesis
?
CO_2
NSC
NSC
BVOC
SM
Aboveground
Belowground
CO_2
NSC
SM
Organ level
CO_2
SM
NSC
NSC
SM
Newly assimilated
Stored

Figure 9. A schematic summary of carbon (C) allocation patterns at the whole-tree and organ level in *Picea abies*. As C availability decreases, transport of newly-assimilated (yellow arrows and boxes) nonstructural carbohydrates (NSC) from aboveground to belowground decreases (dashed line). As a result, locally stored NSC (blue arrows and boxes) are depleted, causing reduced respiratory activity and constrained production of secondary metabolites (SM) in roots. Although newly-assimilated sugars are mixed into stored soluble sugar pools, aboveground respiration decreases as CO_2 supply and total NSC decrease, particularly when NSC reach the minimum operational concentrations (*c*. 25% of control) necessary for survival. Both newly-assimilated and stored NSC contribute to growth but only up to a threshold (*c*. 45% of control) below which operational NSC storage and survival may be compromised. The production of SM of aboveground (yellow-blue) is prioritized over NSC storage and growth, resulting in relatively constant emissions of biogenic volatile organic compounds (BVOCs). C pool dynamics at organ level revealed that little newly-assimilated C is allocated to SM in old organs, and stored SM cannot be mobilized or metabolized in old branches; however, NSC stored in old organs can be mobilized to young organs and provide, along with newly-assimilated NSC, substrates for growth and maintenance of NSC concentrations and the production of SM.

addressing the regulatory mechanisms in long-lived trees where the genome is largely unknown, remains a major challenge that requires combining interdisciplinary approaches including ecological field manipulations, biochemical assays and molecular tools.

Acknowledgements

We thank Savoyane Lambert and Jessica Heublein for their help with sample collection and processing, Olaf Kolle and René Schwalbe for their help with [CO_2] manipulation. Agnes Fastnacht helped us in the greenhouse, Iris Kuhlmann and Anett Enke supported us in the laboratory. Heiko Moossen and Heike Geilmann carried out isotope measurements. J.H. was funded by Chinese Scholarship Council and Max Planck Institute for Biogeochemistry, and acknowledges support from the International Max Planck Research School for Global Biogeochemical Cycles.

Author Contribution

H.H., J.H., S.T., A.H., T.B., J.G., G.G., N.M.v.D and A.S. contributed to the plan and design of the work. J.H. performed experiments, M.R. and A.H. conducted analysis of secondary metabolites, A.W. conducted analysis of volatiles. J.H. analysed the data. J.H. wrote the manuscript with assistance of H.H. All authors contributed to revisions.

Reference

Achard P, Gong F, Cheminant S, Alioua M, Hedden P, Genschik P. 2008. The cold-inducible CBF1 factor-dependent signaling pathway modulates the accumulation of the growth-repressing DELLA proteins via its effect on gibberellin metabolism. *The Plant Cell* **20**: 2117-2129.

Anderegg WRL, Callaway ES. 2012. Infestation and hydraulic consequences of induced carbon starvation. *Plant Physiology* **159**: 1866-1874.

Anderegg WRL, Hicke JA, Fisher RA, Allen CD, Aukema J, Bentz B, Hood S, Lichstein JW, Macalady AK, McDowell N, et al. 2015. Tree mortality from drought, insects, and their interactions in a changing climate. *New Phytologist* **208**: 674-683.

Atkin O. 2015. New Phytologist and the 'fate' of carbon in terrestrial ecosystems. *New Phytologist* **205**: 1-3.

Ayub G, Smith RA, Tissue DT, Atkin OK. 2011. Impacts of drought on leaf respiration in darkness and light in *Eucalyptus saligna* exposed to industrial-age atmospheric CO_2 and growth temperature. *New Phytologist* **190**: 1003-1018.

Ayub G, Zaragoza-Castells J, Griffin KL, Atkin OK. 2014. Leaf respiration in darkness and in the light under pre-industrial, current and elevated atmospheric CO_2 concentrations. *Plant Science* **226**: 120-130.

Brandes E, Kodama N, Whittaker K, Weston C, Rennenberg H, Keitel C, Adams MA, Gessler A. 2006. Short-term variation in the isotopic composition of organic matter allocated from the leaves to the stem of *Pinus sylvestris:* effects of photosynthetic and postphotosynthetic carbon isotope fractionation. *Global Change Biology* **12**: 1922-1939.

Bryant J, Chapin S, Klein D. 1983. Carbon/nutrient balance of boreal plants in relation to vertebrate herbivory. *Oikos* **40**: 357.

Casal JJ. 2013. Photoreceptor signaling networks in plant responses to shade. *Annual Review of Plant Biology* **64**: 403-427.

Chapin FS, Schulze E-D, Mooney HA. 1990. The ecology and economics of storage in plants. *Annual Review of Ecology and Systematics* **21**: 423-447.

Coley PD, Bryant JP, Chapin FS. 1985. Resource availability and plant antiherbivore defense. *Science* **230**: 895-899.

Dietze MC, Sala A, Carbone MS, Czimczik CI, Mantooth JA, Richardson AD, Vargas R. 2014. Nonstructural carbon in woody plants. *Annual Review of Plant Biology* **65**: 667-687.

Eberl F, Hammerbacher A, Gershenzon J, Unsicker SB. 2017. Leaf rust infection reduces herbivore-induced volatile emission in black poplar and attracts a generalist herbivore. *New phytologist.* doi: 10.1111/nph.14565.

Faralli M, Grove IG, Hare MC, Kettlewell PS, Fiorani F. 2017. Rising CO_2 from historical concentrations enhances the physiological performance of *Brassica napus* seedlings under optimal water supply but not under reduced water availability. *Plant, Cell & Environment* **40**: 317-325.

Fatichi S, Leuzinger S, Korner C. 2014. Moving beyond photosynthesis: from carbon source to sink-driven vegetation modeling. *New Phytologist* **201**: 1086-1095.

Fischer S, Hanf S, Frosch T, Gleixner G, Popp J, Trumbore S, Hartmann H. 2015. *Pinus sylvestris* switches respiration substrates under shading but not during drought. *New Phytologist* **207**: 542-550.

Galiano L, Timofeeva G, Saurer M, Siegwolf R, Martínez-Vilalta J, Hommel R, Gessler A. 2017. The fate of recently fixed carbon after drought release: towards unravelling C storage regulation in *Tilia platyphyllos* and *Pinus sylvestris*. *Plant, Cell & Environment* **40**: 1711-1724.

Galvez-Valdivieso G, Fryer MJ, Lawson T, Slattery K, Truman W, Smirnoff N, Asami T, Davies WJ, Jones AM, Baker NR, et al. 2009. The high light response in *Arabidopsis* involves ABA signaling between vascular and bundle sheath cells. *The Plant Cell* **21**: 2143-2162.

Gerhart LM, Harris JM, Nippert JB, Sandquist DR, Ward JK. 2012. Glacial trees from the La Brea tar pits show physiological constraints of low CO_2. *New Phytologist* **194**: 63-69.

Ghannoum O, Phillips NG, Conroy JP, Smith RA, Attard RD, Woodfield R, Logan BA, Lewis JD, Tissue DT. 2010. Exposure to preindustrial, current and future atmospheric CO_2 and temperature differentially affects growth and photosynthesis in *Eucalyptus*. *Global Change Biology* **16**: 303-319.

Gibon Y, Pyl E-T, Sulpice R, Lunn JE, Höhne M, Günther M, Stitt M. 2009. Adjustment of growth, starch turnover, protein content and central metabolism to a decrease of the carbon supply when *Arabidopsis* is grown in very short photoperiods. *Plant, Cell & Environment* **32**: 859-874.

Hammerbacher A, Paetz C, Wright LP, Fischer TC, Bohlmann J, Davis AJ, Fenning TM, Gershenzon J, Schmidt A. 2014. Flavan-3-ols in Norway spruce: biosynthesis, accumulation, and function in response to attack by the bark beetle-associated fungus *Ceratocystis polonica*. *Plant Physiology* **164**: 2107-2122.

Hammerbacher A, Raguschke B, Wright LP, Gershenzon J. 2018. Gallocatechin biosynthesis via a flavonoid 3',5'-hydroxylase is a defense response in Norway spruce against infection by the bark beetle-associated sap-staining fungus *Endoconidiophora polonica*. *Phytochemistry* **148**: 78-86.

Harrison SP, Morfopoulos C, Dani KGS, Prentice IC, Arneth A, Atwell BJ, Barkley MP, Leishman MR, Loreto F, Medlyn BE, et al. 2013. Volatile isoprenoid emissions from plastid to planet. *New Phytologist* **197**: 49-57.

Hartmann H, McDowell NG, Trumbore S. 2015. Allocation to carbon storage pools in Norway spruce saplings under drought and low CO_2. *Tree Physiology* **35**: 243-252.

Hartmann H, Trumbore S. 2016. Understanding the roles of nonstructural carbohydrates in forest trees – from what we can measure to what we want to know. *New Phytologist* **211**: 386-403.

Hartmann H, Ziegler W, Kolle O, Trumbore S. 2013. Thirst beats hunger – declining hydration during drought prevents carbon starvation in Norway spruce saplings. *New Phytologist* **200**: 340-349.

Heil M. 2014. Herbivore-induced plant volatiles: targets, perception and unanswered questions. *New Phytologist* **204**: 297-306.

Herms DA, Mattson WJ. 1992. The dilemma of plants: to grow or defend. *The Quarterly Review of Biology* **67**: 283-335.

Holopainen JK, Gershenzon J. 2010. Multiple stress factors and the emission of plant VOCs. *Trends in Plant Science* **15**: 176-184.

Huang J, Hammerbacher A, Forkelová L, Hartmann H. 2017a. Release of resource constraints allows greater carbon allocation to secondary metabolites and storage in winter wheat. *Plant, Cell & Environment* **40**: 672-685.

Huang J, Reichelt M, Chowdhury S, Hammerbacher A, Hartmann H. 2017b. Increasing carbon availability stimulates growth and secondary metabolites via modulation of phytohormones in winter wheat. *Journal of Experimental Botany* **68**: 1251-1263.

Hunt R. 1982. *Plant growth curves: a functional approach to plant growth analysis.* London, UK: Edward Arnold.

Lewis JD, Ward JK, Tissue DT. 2010. Phosphorus supply drives nonlinear responses of cottonwood (*Populus deltoides*) to increases in CO_2 concentration from glacial to future concentrations. *New Phytologist* **187**: 438-448.

Martin D, Tholl D, Gershenzon J, Bohlmann J. 2002. Methyl jasmonate induces traumatic resin ducts, terpenoid resin biosynthesis, and terpenoid accumulation in developing xylem of Norway spruce stems. *Plant Physiology* **129**: 1003-1018.

Martin DM, Gershenzon J, Bohlmann J. 2003. Induction of volatile terpene biosynthesis and diurnal emission by methyl jasmonate in foliage of Norway spruce. *Plant Physiology* **132**: 1586-1599.

Martínez-Vilalta J, Sala A, Asensio D, Galiano L, Hoch G, Palacio S, Piper FI, Lloret F. 2016. Dynamics of non-structural carbohydrates in terrestrial plants: a global synthesis. *Ecological Monographs* **86**: 495-516.

Massad TJ, Trumbore SE, Ganbat G, Reichelt M, Unsicker S, Boeckler A, Gleixner G, Gershenzon J, Ruehlow S. 2014. An optimal defense strategy for phenolic glycoside production in *Populus trichocarpa* – isotope labeling demonstrates secondary metabolite production in growing leaves. *New Phytologist* **203**: 607-619.

McDowell NG, Ryan MG, Zeppel MJB, Tissue DT. 2013. Improving our knowledge of drought-induced forest mortality through experiments, observations, and modeling. *New Phytologist* **200**: 289-293.

Mithöfer A, Boland W. 2012. Plant defense against herbivores: chemical aspects. *Annual Review of Plant Biology* **63**: 431-450.

Neilson EH, Goodger JQD, Woodrow IE, Møller BL. 2013. Plant chemical defense: at what cost? *Trends in Plant Science* **18**: 250-258.

Palacio S, Hoch G, Sala A, Körner C, Millard P. 2014. Does carbon storage limit tree growth? *New Phytologist* **201**: 1096-1100.

Parducci L, Jørgensen T, Tollefsrud MM, Elverland E, Alm T, Fontana SL, Bennett KD, Haile J, Matetovici I, Suyama Y, et al. 2012. Glacial survival of boreal trees in northern Scandinavia. *Science* **335**: 1083-1086.

Poorter H, Fiorani F, Pieruschka R, Wojciechowski T, van der Putten WH, Kleyer M, Schurr U, Postma J. 2016. Pampered inside, pestered outside? Differences and similarities between plants growing in controlled conditions and in the field. *New Phytologist* **212**: 838-855.

Poorter H, Niklas KJ, Reich PB, Oleksyn J, Poot P, Mommer L. 2012. Biomass allocation to leaves, stems and roots: meta-analyses of interspecific variation and environmental control. *New Phytologist* **193**: 30-50.

R Development Core Team. 2016. *R: A language and environment for statistical computing.* Vienna, Austria: R foundation for Statistical computing, URL http://www.r-project.org. Version 3.3.2.

Reich PB, Hobbie SE, Lee TD. 2014. Plant growth enhancement by elevated CO_2 eliminated by joint water and nitrogen limitation. *Nature Geoscience* **7**: 920-924.

Roberts MR, Paul ND. 2006. Seduced by the dark side: integrating molecular and ecological perspectives on the inflence of light on plant defence against pests and pathogens. *New Phytologist* **170**: 677-699.

Ryan MG, Sapes G, Sala A, Hood SM. 2015. Tree physiology and bark beetles. *New Phytologist* **205**: 955-957.

Sala A, Woodruff DR, Meinzer FC. 2012. Carbon dynamics in trees: feast or famine? *Tree Physiology* **32**: 764-775.

Scanlon JT, Willis DE. 1985. Calculation of flame ionization detector relative response factors using the effective carbon number concept. *Journal of Chromatographic Science* **23**: 333-340.

Schmid S, Palacio S, Hoch G. 2017. Growth reduction after defoliation is independent of CO_2 supply in deciduous and evergreen young oaks. *New Phytologist* **214**: 1479-1490.

Sevanto S, McDowell NG, Dickman LT, Pangle R, Pockman WT. 2014. How do trees die? A test of the hydraulic failure and carbon starvation hypotheses. *Plant, Cell & Environment* **37**: 153-161.

Skirycz A, De Bodt S, Obata T, De Clercq I, Claeys H, De Rycke R, Andriankaja M, Van Aken O, Van Breusegem F, Fernie AR, et al. 2010. Developmental stage specificity and the role of mitochondrial metabolism in the response of *Arabidopsis* leaves to prolonged mild osmotic stress. *Plant Physiology* **152**: 226-244.

Tomonori T, Sebastian K, M. DN. 2017. Root and shoot glucosinolate allocation patterns follow optimal defence allocation theory. *Journal of Ecology* **105**: 1256-1266.

Trumbore S, Brando P, Hartmann H. 2015. Forest health and global change. *Science* **349**: 814-818.

Ullah C, Unsicker SB, Fellenberg C, Constabel CP, Schmidt A, Gershenzon J, Hammerbacher A. 2017. Flavan-3-ols are an effective chemical defense against rust infection. *Plant Physiology* **175**: 1560-1578.

Unsicker SB, Kunert G, Gershenzon J. 2009. Protective perfumes: the role of vegetative volatiles in plant defense against herbivores. *Current Opinion in Plant Biology* **12**: 479-485.

van Dam NM, Bouwmeester HJ. 2016. Metabolomics in the rhizosphere: tapping into belowground chemical communication. *Trends in Plant Science* **21**: 256-265.

Vickers CE, Gershenzon J, Lerdau MT, Loreto F. 2009. A unified mechanism of action for volatile isoprenoids in plant abiotic stress. *Nature Chemical Biology* **5**: 283-291.

Way DA, Ghirardo A, Kanawati B, Esperschütz J, Monson RK, Jackson RB, Schmitt-Kopplin P, Schnitzler J-P. 2013. Increasing atmospheric CO_2 reduces metabolic and physiological differences between isoprene- and non-isoprene-emitting poplars. *New Phytologist* **200**: 534-546.

Weber R, Schwendener A, Schmid S, Lambert S, Wiley E, Landhäusser SM, Hartmann H, Hoch G. 2018. Living on next to nothing: tree seedlings can survive weeks with very low carbohydrate concentrations. *New Phytologist* **218**: 107-118.

Wiley E, Casper BB, Helliker BR. 2017a. Recovery following defoliation involves shifts in allocation that favour storage and reproduction over radial growth in black oak. *Journal of Ecology* **105**: 412-424.

Wiley E, Helliker B. 2012. A re-evaluation of carbon storage in trees lends greater support for carbon limitation to growth. *New Phytologist* **195**: 285-289.

Wiley E, Hoch G, Landhäusser SM. 2017b. Dying piece by piece: carbohydrate dynamics in aspen (*Populus tremuloides*) seedlings under severe carbon stress. *Journal of Experimental Botany* **68**: 5221-5232.